

Received 26 November 2023, accepted 15 December 2023, date of publication 18 December 2023,
date of current version 27 December 2023.

Digital Object Identifier 10.1109/ACCESS.2023.3344640

RESEARCH ARTICLE

NLOS Identification for UWB Positioning Based on IDBO and Convolutional Neural Networks

QIANKUN KONG 

Wuxi River Water Diversion Project Management Center, Quzhou 324000, China


e-mail: sjnmmbrnhk@yeah.net

ABSTRACT Ultra-wideband (UWB) is regarded as the technology with the most potential for precise indoor location due to its centimeter-level ranging capabilities, good time resolution, and low power consumption. However, Because of the presence of non-line-of-sight (NLOS) error, the accuracy of UWB localization deteriorates significantly in harsh and volatile indoor conditions. Therefore, identifying NLOS conditions is crucial to enhancing the accuracy of UWB location. This paper proposes a convolutional neural network (CNN) classification method based on an improved Dung Beetle Optimizer (DBO). Firstly, based on the standard DBO, the Circle chaotic mapping, non-uniform Gaussian variational strategy, and multi-stage perturbation strategy are used to optimize the exploration capability and enhance the performance of original DBO method, the superiority-seeking ability of IDBO is demonstrated by testing 23 benchmark functions. In addition, based on the IDBO algorithm, we propose an IDBO-CNN classification model, with the help of IDBO, the accuracy of NLOS identification is improved by adjusting the hyperparameters of CNN to be closer to the optimal solution. Experiments conducted on the open-source dataset demonstrate that IDBO-CNN is capable of achieve the desired effect. In comparison to the conventional CNN approach, the F1-score achieved by IDBO-CNN is enhanced by 3.31%, which demonstrates that IDBO-CNN has superior identification accuracy.

INDEX TERMS UWB localization, NLOS identification, IDBO, circle chaotic mapping, non-uniform Gaussian variation, multi-stage dynamic disturbance, CNN.

I. INTRODUCTION

The advancement of the Internet of Things technology has revolutionized the way we live, more and more people are becoming interested in location-based services in indoor environments, this is because most of the human activities take place indoors. UWB, acoustic [1], ZigBee [2], infrared [3], visible light communication (VLC) [4], radio frequency identification (RFID) [5], and hybrid positioning systems employing multiple technologies are the most popular indoor positioning methods at the moment. It is generally agreed that the UWB technology is the most promising technique for accurate location among these several technologies due to its good time resolution, centi-meter-level ranging capabilities, low power consumption, great penetration, and good anti-multipath effect, and other advantages.

The associate editor coordinating the review of this manuscript and approving it for publication was Yafei Hou .

As a time of arrival (TOA) based approach, the UWB-based positioning system has centimeter-level positioning accuracy, however, its positioning performance deteriorates sharply under indoor non-line-of-sight (NLOS) propagation conditions [6]. NLOS is a common phenomenon in wireless signal transmission, as shown in Fig. 1, where the direct signal transmission path between anchor and tag is obstructed or blocked by the barriers (furniture, wall, goods, glass window, e.g.). In this situation, the signal between the transmitter and the receiver may be propagated through multiple paths, such as diffraction, reflection, refraction, and penetration [7], consequently, the distance estimated based on whether TOA or received signal strength indicator (RSSI) is biased. NLOS propagation can be observed in a variety of positioning situations in production and daily life, such as indoor navigation, asset tracking, etc. It is worth mentioning that UWB positioning is usually located by range-based methods such as TOA or time difference of arrival (TDOA), which has high-ranging accuracy, so NLOS propagation has

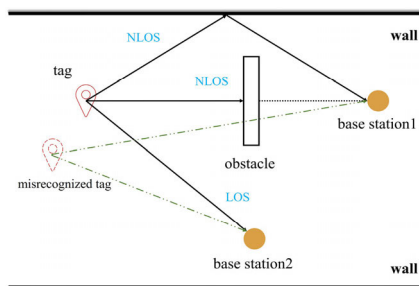


FIGURE 1. LOS and NLOS propagation in the UWB-based system.

a more serious impact on the UWB positioning system. Therefore, high-precision positioning technology must find a solution to the crucial issue of how to identify and correct NLOS errors.

In recent years, researchers have proposed many methods to NLOS identification and mitigation, these methods are mainly divided into traditional methods, machine learning-based methods, and deep learning-based methods. Traditional LOS/NLOS identification method using characteristic parameters of transmission channel, such as the Rice factor, kurtosis, skewness, mean excess delay (MED), etc. this method accuracy is not high and is only suitable for static environment. The method based on machine learning requires manual extraction of useful information from UWB signals, which require much human labor. The methods based on deep learning generally adopt convolutional neural networks (CNN), residual network (ResNet) and its combination with other technologies, current research mainly focuses on the CNN network structure, ignoring the influence of model parameters on the recognition rate. To solve the above problems, this paper proposes a CNN identification method based on an improved Dung Beetle Optimizer (IDBO), IDBO was used to optimize CNN parameters and improve recognition rate. In summary, this paper makes following contributions:

(1) Aiming at the shortcoming of standard DBO, the circle sequence, non-uniform Gaussian mutation and multi-stage dynamic perturbation strategy are used to increase the search space of the algorithm and avoid local optimality.

(2) The benchmark function of CEC2017 is used as the fitness function, including unimodal, multimodal, separable and indivisible. Through Wilcoxon rank sum test and sensitivity analysis, it is proved that IDBO has strong optimization ability and fast convergence speed.

(3) Simulations using channel impulse response (CIR) data sets show that the IDBO-CNN model does a better job of identifying NLOS, the identification performance of the suggested IDBO-CNN model is compared with the existing CNN model, which shows that the proposed IDBO-CNN model has better feature extraction and identification abilities for NLOS signals.

The structure of this paper are as follows: The various related works pertaining to NLOS classification are discussed in Section II. The fundamental concepts of CNN and DBO are introduced in Section III, and elaborates the model of

IDBO. In Section IV, the validity of the suggested IDBO is tested and assessed by benchmark functions. Section V utilizes open-source data sets to verify and test the validity and feasibility of NLOS identification based IDBO-CNN. Finally, we wrap up the study and talk about further research in Section VI.

II. RELATED WORK

A. NLOS IDENTIFICATION

To enhance indoor location accuracy, many scholars have discussed several NLOS identification methods from different perspectives, and current NLOS identification can be split into three categories according to the basic algorithm used: traditional methods, machine learning-based methods, and deep learning-based methods [8].

Traditional NLOS identification methods can be divided into three categories, namely statistics-based methods [7], [9], range-based methods [10], location-based methods [11]. Statistics-based methods use the probability density function (PDF) or the statistical features of CIR, such as the Rice factor, kurtosis, skewness, MED for NLOS identification. This method usually needs to extract UWB signal features and set a reasonable threshold, but the appropriate threshold is difficult to determine [12] and easy to be affected by the environment [8]. Range-based methods use variance of range estimates or PDF of the received signal to identify NLOS, this method requires a lot of distance measurements, therefore not suitable for application in real-time UWB positioning system. Location-based methods identify NLOS by comparing external environment information (maps, geometric location, path continuity) [11] with different subsets of actual ranging estimates, which are not suitable for indoor scenes with large changes. In summary, traditional methods are limited by prior knowledge or the existence of time delays, or it is difficult to determine the appropriate distribution function or additional constraints are required.

Machine learning includes random forests (RF) [13], decision trees (DT) [14], and other methods, these methods need to manually extract UWB CIR characteristics and establish the relationship between signal features and LOS/NLOS propagation through supervised learning. In Reference [15], an NLOS identification method with fuzzy credibility-based support vector machines (FC-SVM) and dynamic threshold comparison (DTC) is proposed, this is done in two steps, starting with a coarse-grained NLOS classification using the DTC approach, then moving on to a fine-grained result using FC-SVM. A UWB positioning system based on RF is proposed in Reference [16], the RF algorithm is innovatively applied to Kalman filter measurement update, and the Taylor algorithm is adopted to improve the estimation accuracy. To address the performance degradation caused by the disproportionate number of LOS and NLOS signals, Che et al. [17] proposed the Weighted Naive Bayes algorithm to reduce the impact of the limited number of NLOS components on the train the model. The recognition effect of the method based on machine learning largely depends on offline data collecting

and labeling, and selection of channel statistical characteristics. However, some deep-level features are unknown to human beings, the collection and labeling of offline data consume a lot of manpower and are not suitable for dynamic indoor environment, which limits the further improvement of recognition performance of machine learning methods.

In recent years, deep learning has developed rapidly in image processing, natural language processing, etc. Deep learning techniques are capable of learning complicated, non-linear and high-dimensional features from massive CIR data, it has been introduced into NLOS identification by researchers and has achieved promising results. The research mainly focuses on CNN [18], temporal convolutional networks (TCN) [19], Long Short-Term Memory (LSTM) [20], and the combination of different technologies [21]. Cui et al. [22] presents a LOS/NLOS classification technique based on CNN and Morlet wave transformation, which can identify NLOS scenarios in time-frequency domain, but this technique is more suitable for deployment in static scenes. In Reference [23], a network that combines the TCN and attention mechanisms with the CIR as its input is proposed to be used to detect NLOS propagation. The particle swarm optimization (PSO) method is utilized choose the network's main parameters, resulting in improved accuracy and a faster processing speed. The UWB positioning system described in Reference [20] employs LSTM and uses the CIR of the UWB signal received to differentiate between LOS and NLOS conditions. Generative Adversarial Networks (GAN) are used in Reference [24] to produce diagnostic information for frame transmission under NLOS circumstances, then, NLOS situations are identified using CNN. In Reference [25], the LSTM is used to identify LOS/NLOS situations using the combined channel features, which are made up of four characteristics of channel state information (CSI) and CIR. A reliable approach for identify NLOS utilize fuzzy decision tree (FDT) that is based on Bayesian optimization is presented in Reference [26], this technique extracts the classification characteristics from CIR, generates FDT with Bayesian optimization, and detects the propagation circumstances of the UWB signal. Deep learning technology has developed rapidly in NLOS identification, but it also has some shortcomings. The current research focuses on the adjustment and optimization of the CNN model structure, ignoring the influence of the model hyperparameters on the identification performance, which is one of the key factors affecting the model performance.

B. PARAMETER OPTIMIZATION

Before the CNN model is applied to NLOS recognition, the internal hyperparameters must be set, which is one of the key factors affecting the performance of the model [27]. Although genetic algorithm (GA) and PSO have some effects in parameter optimization, their search in hyperparameter space is often inefficient. In contrast, DBO [28] is a new meta-heuristic algorithm and has strong search ability and

fast convergence speed, which can optimize CNN parameters more effectively. Some scholars have begun to study using DBO to optimize CNN parameters. Yuan et al. [27] introduced a new water-body detection method, which established a DBO-CNN model and used the DBO algorithm to optimize hyperparameter of CNN model to improve detection performance. Guo et al. [29] proposed a DBO-CNN model, which automatically adjusts CNN hyperparameters to identify speakers. By testing the data set of 50 people, it is proved that the average recognition rate of this method is improved by 1.22~4.39%. Zhao et al. [30] proposed a combined traffic flow prediction model. Firstly, an improved IDBO algorithm is used to optimize LSTM parameters, then the predicted value of the subsequence is recombined to get the final result, indicating that IDBO-LSTM improves the accuracy of prediction. Zhang and Zhu [31] improved the DBO algorithm with three strategies, and then optimized a back-propagation (BP) neural network with IDBO algorithm, proving that IDBO-BP has a superior performance in predicting the parameters of heat treated larch sawed timber. By using DBO algorithm to automatically iteratively search the optimal LSTM parameters, Zhang et al. [32] proposed a short-term power load combination prediction model of DBO-LSTM, the average prediction error was reduced by 25.13%. However, every meta-heuristic algorithm has its limitations and cannot solve all problems. Due to the randomness of DBO algorithm, it may lead to local optimization, so there is still room for improvement.

To resolve the problems above, a new IDBO algorithm is proposed to optimize CNN parameters by using several strategies. Simulation results show that the CNN classifier with optimized parameters can identify NLOS conditions more accurately in complex indoor environments, compared with existing state-of-the-art algorithms.

III. MODELS AND ALGORITHMS

A. CONVOLUTIONAL NEURAL NETWORK

The main feature of CNN is convolutional operation, the main steps of CNN are as follows: (1) extraction of initial features by the convolutional layer; (2) extraction of main features by the pooling layer; (3) aggregation of various features by the fully connected layer; and finally, classification prediction.

(1) Convolutional layer: Convolution in CNN is to calculate the product of each element point in the input data matrix with the corresponding element point in the coverage of the convolution kernel matrix and add up all the products, the cumulative sum is the output obtained from each convolution operation (feature graph).

(2) Pooling layer: The purpose of the pooling layer is to decrease the dimensionality of the data while preserving the characteristics of the resulting feature graph. In essence, the pooling layer divides the feature graph generated by convolution into multiple non-overlapping $n \times n$ regions, and uses the sliding window to slide through each region successively and pool the elements within the region. This paper adopts maximum pooling.

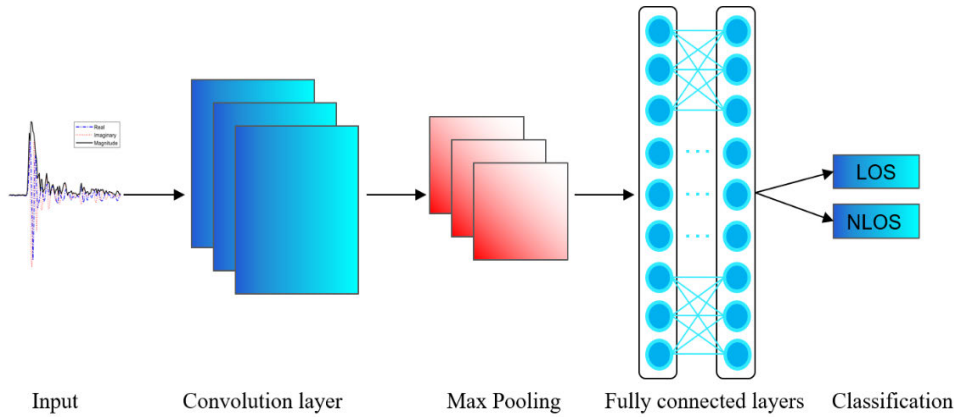


FIGURE 2. CNN structure.

(3) Fully connected layer: Operations such as the convolution layer and pooling layer in CNN are equivalent to mapping the input data to the feature space, while the full connection layer is equivalent to mapping the previously obtained features to the sample space. The fully connected layer concatenates all the features of the input data into a one-dimensional feature space. A weighted summation of the fully connected layer inputs and an activation function can obtain the corresponding output.

B. DBO ALGORITHM

The DBO was suggested based on the behavior of dung beetles, which roll, dance, forage, steal, and breed [28]. This algorithm introduces certain techniques, such as identifying the direction of advancement based on dance behavior. With respect to convergence time and solution accuracy, this algorithm is competitive with existing optimization techniques. The four DBO behaviors are listed below:

1) ROLLING BALL

Dung beetles roll huge dung balls, they make the ball travelling in a line by using the sun as a guide. As it rolls, the rolling dung beetle alters its position in accordance with the equation:

$$x_i(t + 1) = x_i(t) + \alpha \times k \times x_i(t - 1) + b \times \Delta x$$

$$\Delta x = |x_i(t) - X^w| \tag{1}$$

where, the iteration count is denoted by t , the location of the i -th beetle during the t -th iteration is represented by $x_i(t)$. a constant parameter denoting the deviation factor is $k \in (0, 0.2]$, $b \in (0, 1)$ is a fixed constant, the value of α is 1 or -1 , X^w and Δx are the worst location and light brightness variation, respectively.

Dung beetles encounter obstacles, they must dance to reposition themselves and find another way. To imitate this dancing action, a tangent function is employed. The ball is kept rolling backwards until the dung beetle decides on a new direction. the following is the dung beetle's position formula:

$$x_i(t + 1) = x_i(t) + \tan(\theta) |x_i(t) - x_i(t - 1)| \tag{2}$$

where, θ represents the deflection angle and $[0, \pi]$ indicates the value of the variable.

2) SPAWNING

Female dung beetles hide dung balls in a safe area to lay their eggs in nature. Motivated by this action, the following methodology of selecting boundaries is used to imitate the dung beetle oviposition area:

$$Lb^* = \max(X^* \times (1 - R), Lb)$$

$$Ub^* = \min(X^* \times (1 + R), Ub) \tag{3}$$

where X^* indicates the location that is currently the most optimal, the lower and upper boundaries of the oviposition area are denoted by Lb^* and Ub^* , $R = 1 - t/T_{max}$, T_{max} represents the maximum number of iterations, the optimization problem's upper bounds and lower bounds are denoted by Lb and Ub .

The female beetle will choose an egg to lay in the designated oviposition area once it has been identified. According to Equation (3), the value of R will primarily determine how dynamically the oviposition area's boundary range changes. During iteration, the egg's position dynamically changes, as specified as:

$$X_i(t + 1) = X^* + b_1 \times (X_i(t) - Lb^*) + b_2 \times (X_i(t) - Ub^*) \tag{4}$$

where the location of the i -th egg in the t -th iteration is indicated by $X_i(t)$, the two stochastic vectors b_1 and b_2 not connected with one another and have dimensions of $1D$. The optimization problem's size is D .

3) FORAGING

Female beetle eggs hatch and expand throughout time, in search of food, some grown small beetles will emerge from the soil, the optimum foraging habitat for small beetles is depicted below:

$$Lb^b = \max(X^b \times (1 - R), Lb)$$

$$Ub^b = \min(X^b \times (1 + R), Ub) \tag{5}$$

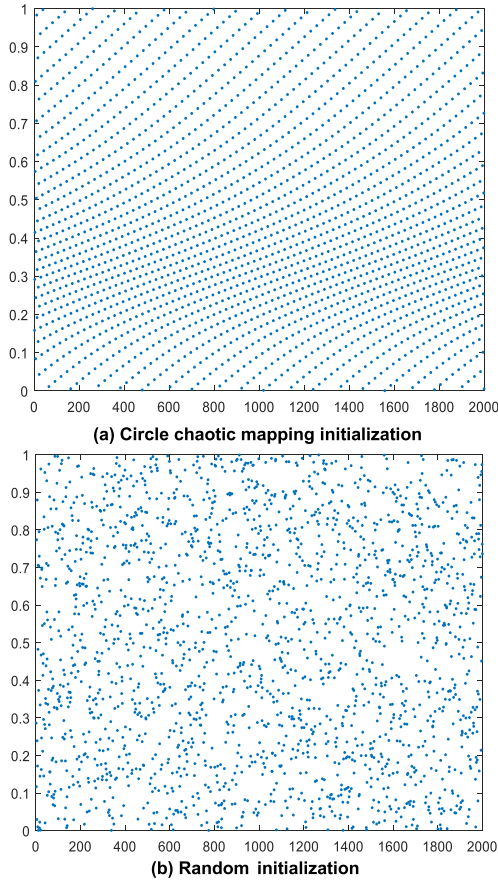


FIGURE 3. Comparison of random generation method and circle chaotic mapping method (a) Circle chaotic mapping initialization; (b) Random initialization.

X^b is the global optimal position, the lower and upper boundaries of the ideal foraging area are denoted by Lb^b and Ub^b , as a result, The following is an updated description of the little dung beetle's location.

$$x_i(t+1) = x_i(t) + C_1 \times (x_i(t) - Lb^b) + C_2 \times (x_i(t) - Ub^b) \quad (6)$$

where $x_i(t)$ denotes the little dung beetle's location at the t -th iteration. C_1 stands for normal-distributed random variable, C_2 is a random vector that ranges from 0 to 1.

4) STEALING

Some beetles are known as thieves because they take other beetles' dung balls. Since X^b is the ideal food supply according to Equation (5), it follows that the location around X^b is the best area for competitive food. The thief's location is updated as follows during the iteration process:

$$x_i(t+1) = X^b + S \times g \times \left(|x_i(t) - X^*| + |x_i(t) - X^b| \right) \quad (7)$$

where $x_i(t)$ denotes the thief's position at the t -th iteration. the value of s is fixed constant, while g is a 1-dimensional random vector that follows a normal distribution.

C. IMPROVED DBO

The traditional DBO algorithm has several drawbacks, including limited global searchability and the tendency to fall into local optimality, this research suggests a more effective dung beetle optimizer to overcome these shortcomings.

1) CIRCLE CHAOTIC MAPPING

In the original DBO algorithm, random population initialization is adopted, which may lead to insufficient population diversity and excessive convergence in subsequent iterations. A metaheuristic algorithm's population diversity can be increased by using chaotic sequences because of their randomness and ergodicity [33]. The fundamental strategy utilizes chaos models to map chaotic sequences into individual search areas, such as Kent [34], Tent [35] or Logistic [36] chaos mapping.

When choosing a chaotic map, two important properties must be considered: simplicity and ergodicity. Due to its uniform phase distribution and straightforward Equations, piecewise linear chaotic mapping satisfies these requirements. In this paper, a random sequence is produced via circle chaotic mapping, the following is the formula:

$$x_{i+1} = \text{mod} \left(x_i + 0.2 - \left(\frac{0.5}{2\pi} \right) \sin(2\pi x_i), 1 \right) \quad (8)$$

Particle distribution using Circle mapping in (a) is more uniform than random distribution in (b), avoiding the situation where there are fewer dung beetle populations near the optimal solution. The initial position distribution of the improved population was more uniform, which expanded the search scope of dung beetle groups in space, increased the diversity of group positions, and fixed the algorithm's flaw of being susceptible to local extreme values, thus enhance the optimization efficiency of the DBO algorithm.

2) MULTI-STAGE DYNAMIC DISTURBANCE STRATEGY

The rolling ball process can enhance the search randomness and the population diversity, but the solution of the new individual dung beetle may not be accurate and may be prone to noise, which may negatively affect the search effect of the DBO algorithm. In this article, a multi-stage dynamic perturbation strategy is proposed for the rolling ball process to update the optimal solution position by stage dynamic perturbation to avoid falling into local optimal. Its formula is shown in (9):

$$x_i(t+1) = N(x_i(t), \sigma) \quad (9)$$

where σ represents the uncertainty relative to $x_i(t+1)$ and is non-increasing function with t iterations, this is its modified formula:

$$\sigma = \begin{cases} \sigma_1 & , t < \alpha_1 T \\ \sigma_1 - \frac{(\sigma_1 - \sigma_2)(t - \alpha_1 T)}{(\alpha_2 T - \alpha_1 T)} & \alpha_1 T < t < \alpha_2 T \\ \sigma_2 & , t > \alpha_2 T \end{cases} \quad (10)$$

TABLE 1. Major notations used in this paper.

Notation	Definitions
t	Number of iterations
θ	Angle of deflection
Δx	Variation of brightness
Lb^*	Lower boundaries of the oviposition area
Ub^*	Upper boundaries of the oviposition area
T_{max}	Maximum number of iterations
Lb	Lower bounds of the optimization problem
Ub	Upper bounds of the optimization problem
X^w	The global worst location
X^b	The present optimum location
R	The edge of ovipositional region
D	Dimension of the optimization problem
σ	Radius parameter of the normal disturbance
$\Delta(t, GD_t^i)$	Step size of non-uniform variation

where, α represents the radius parameter of the normal disturbance to the original optimal dung beetle position, and $\sigma_1 < \sigma_2$; in this paper, $\alpha_1 = 0.000001$, $\sigma_2 = 0.9$; α_1, α_2 are the control parameters of the change of radius; and $\alpha_1 < \alpha_2$, in this paper, $\alpha_1 = 0.4$, $\alpha_2 = 0.7$; the iterations number is t , and the maximum iterations number is T .

3) NON-UNIFORM GAUSSIAN VARIATION STRATEGY

The spawning process refers to the iterative process of the algorithm, in which dung beetles exchange information and merge updates to speed up the search speed and expand the search space. This process can be separated into two steps: information exchange and information merging. Information merging may result in multiple dung beetles merging with each other, but the resulting individual solution may not be as good or worse than the original one. This may cause the solution set of the algorithm to shrink and the search efficiency to decrease. In this paper, we propose a non-uniform Gaussian variation strategy for the reproduction process, namely:

$$x_i(t + 1) = x_i(t) + \Delta(t, GD_t^i) \tag{11}$$

$$\Delta(t, y) = y \left(1 - r \left(\frac{1-t}{T_{max}} \right)^b \right) \tag{12}$$

$$GD_t^i = N \left((F - x_j^i), \sigma \right) \tag{13}$$

where, $\Delta(t, GD_t^i)$ is the step size of non-uniform variation, it is a mutation operator that adaptively adjusts the step size by Gaussian distribution (GD_t^i); r is a uniformly generated random number within the range of 0 to 1; b is a system parameter, determines the uniformity of variation

calculations, values for $b = 2$; F is the target position; The Gaussian distribution has a standard deviation denoted by σ .

The non-uniform Gaussian variation strategy has the following characteristics: 1) The update object is the dung beetle with the worst fitness in the population, instead of all the individuals in the current population, which reduces the complexity; 2) As can be seen from Equation (9), the update formula takes the individual itself as the basis, selects the information merging object and the current individual for Gaussian distribution, and adaptively adjusts the learning strategy of variation step length. This approach to updating is helpful for sustaining population variety and enhancing the global search capability of the algorithm.

D. IDBO ALGORITHM FRAMEWORK AND COMPLEXITY ANALYSIS

Assuming that N, M, D represents the population size, the problem dimension and the maximum number of iterations, respectively. The time complexity of the initial phase is $C1 = O(N * D)$ and the complexity during iteration is $C2 = O(M * N * D)$, so the complexity of the DBO is $C1 + C2$ which is $O(N)$. IDBO does not use greedy strategies, reverse learning, etc., which would add complexity, the complexity of IDBO algorithm is $O(N)$ in both the initialization stage and the rolling stage. Assuming that spawning dung beetles account for $P\%$, so the complexity of the spawning stage is $O(P * M * N * D)$, The total complexity is $O(N)$, so the IDBO has the same complexity as the DBO algorithm [37].

Algorithm IDBO Algorithm

Require: The maximum iteration, the size of the particle's population N . Obtain an initialized population using circle chaotic mapping strategy.

Ensure: Optimal position X^b and its fitness value.

- 1: Initialize the particle's population $i \leftarrow 1, 2, \dots, N$ and define its relevant parameters
- 2: **while** \leq **do**
- 3: for $i = 1$ to Number of rolling dung beetles **do**
- 4: $\alpha = rand(1)$
- 5: **if** ≤ 0.9 **then**
- 6: Update Rolling Dung Beetle Location by Eq. (1).
- 7: **else**
- 8: Rolling the ball in the encounter of obstacles by Eq. (9) and Eq. (10) to update.
- 9: **end if**
- 10: **end for**
- 11: The value of the nonlinear convergence factor is calculated by $R = 1 - t/T_{max}$.
- 12: **for** $i = 1$ to Number of Spawning dung beetles **do**
- 13: Updating of Spawning dung beetles by Eq. (10), Eq. (11) and Eq. (12).
- 14: **end for**
- 15: **for** $i = 1$ to Number of Foraging dung beetles **do**
- 16: Updating of foraging dung beetles by Eq. (5) and Eq. (6).
- 17: **end for**
- 18: **for** $i = 1$ to Number of Stealing dung beetles **do**
- 19: Updating of stealing dung beetle by Eq. (7).
- 20: **end for**
- 21: **end while**
- 22: Return X^b and its fitness value f_b ;



FIGURE 4. Optimization process of CNN parameters using IDBO algorithm.

E. CNN METHOD BASED ON IDBO OPTIMIZATION

The NLOS identification model is established in this research using the CNN approach, however, it is challenging to determine the ideal hyperparameter combination for a given task because CNN has many hyperparameters. Using past empirical methods to replicate the parameter values used in other problems, or to find the best value through trial and error will consume a lot of cost and time, and may not be the optimal solution. Therefore, the IDBO-CNN is suggested in this paper, the essence of IDBO-CNN is to adjust the hyperparameters of CNN to the optimal solution by using the fast convergence rate and accurate global search ability of IDBO, so as to enhance identification accuracy. Fig. 4 shows the IDBO-CNN procedure, the following is the major procedures:

(1) IDBO algorithm initialization, including the population size, the percentage of dung beetles' four behaviors, variable parameter dimension, maximum iterations (T_{\max}), and upper and lower bounds (Lb , Ub).

(2) Initialize each dung beetle's location.

(3) Record the global optimum position after the fitness values are calculated. In this research, we develop the fitness function by computing the disparity between the true and forecasted values using Mean Square Error, the following is

the formula:

$$MSE = \frac{1}{n} \sum_i^n (\hat{y}_i - y_i)^2 \quad (14)$$

(4) Update each dung beetle's location as follows: for the rolling dung beetle, move it in obstacle-free mode or dance in obstacle mode using Equations (1) or Equations (2); for the breeding dung beetle, calculate its location Equations (11), Equations (12), and Equations (13); for a foraging dung beetle, calculate its location using Equations (5) and Equations (6); for the thieving dung beetle, calculate its location using Equation (7).

(5) After the update, check whether each dung beetle's location surpasses Lb and Ub . If so, repeat step 3. Otherwise, continue to execute.

(6) Updated optimal solution and value.

(7) Repeating Steps 3, 4, 5, and 6 until the maximum iteration count is reached, and then feed the parameters into the CNN model.

IV. RESULTS ANALYSIS

In this section, through a set of simulation experiments employing benchmark functions, the efficacy of the IDBO method is evaluated.

TABLE 2. Benchmark function.

Function	Dim	Range	Fmin
f_1 Sphere	10	[-100, 100]	0
f_2 Schwefel 1.2	10	[-30, 30]	0
f_3 Schwefel 2.21	30	[-100, 100]	0
f_4 Quartic	30	[-100, 100]	0
f_5 Rosenbrock	30	[-30, 30]	0
f_6 Step	50	[-100, 100]	0
f_7 Schaffer	50	[-100, 100]	0
f_8 Foxholes	10	[-10 10]	0
f_9 Kowalik	10	[-5.12 5.12]	0
f_{10} Rastrigin	30	[-10 10]	0
f_{11} Ackley	30	[-50 50]	0
f_{12} Griewank	10	[-50 50]	0
f_{13} Penalized1	30	[-100 100]	-12569
f_{14} Penalized2	10	[-5.12 5.12]	0
f_{15} Kowalik	10	[-50 50]	0
f_{16} Camel-Back	10	[-100 100]	0
f_{17} Branin	30	[-50 50]	0
f_{18} Goldstein	30	[-50 50]	0
f_{19} Hartman1	30	[-5 5]	-3
f_{20} Hartman2	4	[-5 5]	-3
f_{21} Shekel1	2	[0 10]	-1
f_{22} Shekel2	2	[0 10]	-1
f_{23} Shekel3	2	[0 10]	-1

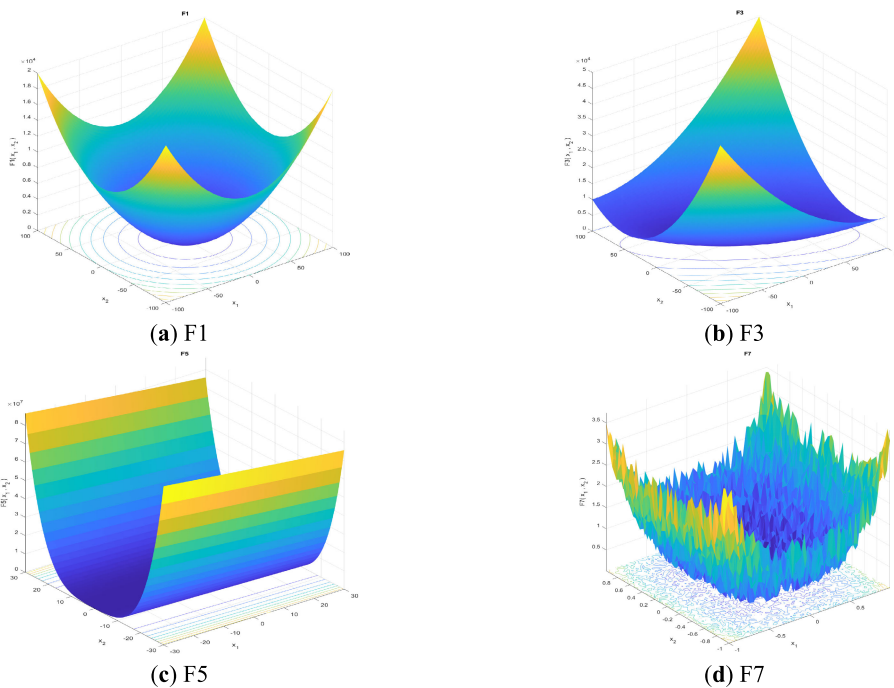


FIGURE 5. 3D view of partial unimodal functions.

A. BENCHMARK FUNCTIONS FOR OPTIMIZATION

To evaluate the IDBO optimization algorithms, twenty-three test functions, previously published in [38] and [39],

were selected. We evaluated the convergence time and accuracy of the method using the unimodal test functions F1–F7, which possess a unique global optimal solution.

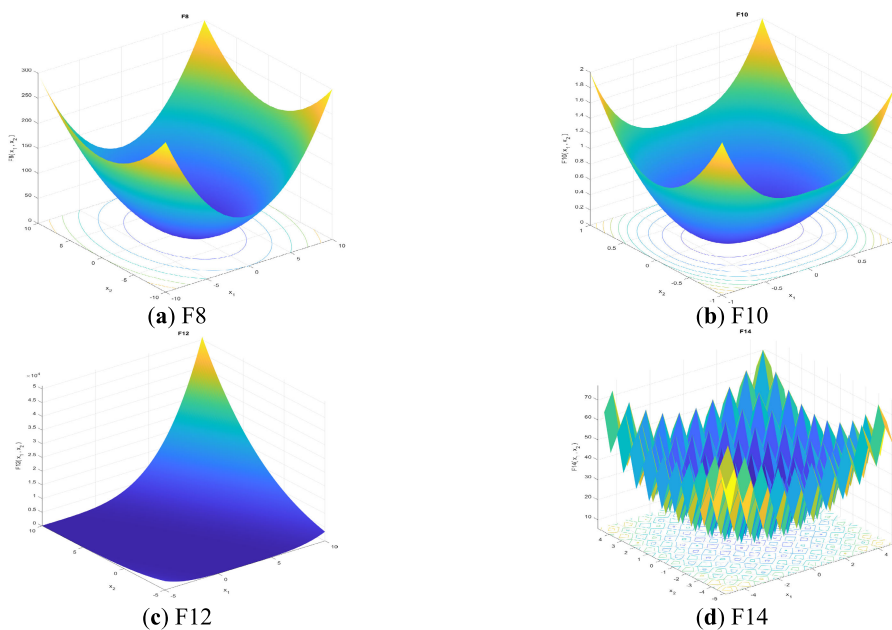


FIGURE 6. 3D view of partial multimodal functions.

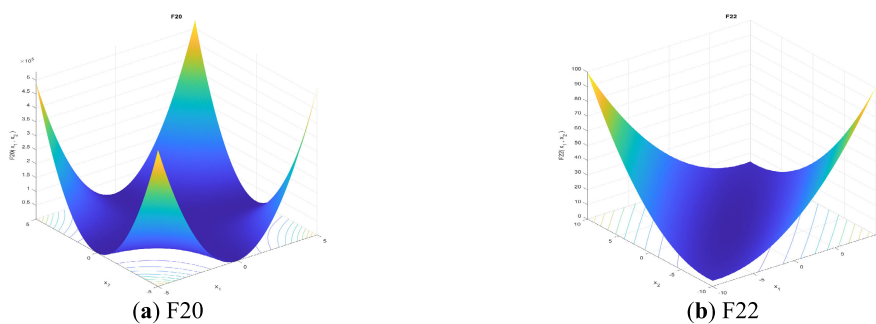


FIGURE 7. 3D view of partial multimodal functions with fix dimension.

TABLE 3. Benchmark function.

Algorithm	Parameter	Setting
EHO	α and β	0.5 and 0.1
WOA	a	from 2 to 0
GWO	a	from 2 to 0
CLPSO	c_1 and c_2	2
	Inertia weight	Linearly decreased from 0.9 to 0.1
DBO	α and β	0.1
	a and b	0.3 and 0.5
IDBO	α and β	0.1
	a and b	0.3 and 0.5

The global search of the method was evaluated using the multimodal test functions F8–F14, which have one global optimum solution and many local optimal solutions. Multimodal test functions for the functions F14–F23 with fixed dimensions. The dimensions, search ranges, and theoretical optimum solutions of these benchmark test functions are listed in Table 2. To make these test functions

and their optimum solution easier to understand, some of these functions are seen in three-dimensional form in Figs. 5, 6, and 7.

B. PARAMETER SETTINGS

Since the DBO algorithm has fewer variants, to assess its reliability, we compare IDBO with five other fundamental

TABLE 4. Benchmark function optimization results.

Function	Index	IDBO	DBO	GWO	WOA	CLPSO	EHO
F1	Best	2.56E-85	6.14E-68	2.11E-27	3.10E-39	1.50E-12	4.96E+01
	Mean	9.37E-65	1.14E-34	3.46E-25	1.86E-34	6.50E-05	1.94E+02
	STD	2.47E-64	3.51E-34	7.72E-25	5.99E-34	1.36E-04	1.10E+02
F2	Best	2.91E-43	6.22E-40	1.28E-15	1.91E-24	9.83E-01	1.59E+00
	Mean	1.17E-32	3.02E-22	6.96E-15	1.98E-22	2.26E+00	2.75E+00
	STD	3.58E-32	1.12E-21	7.50E-15	4.34E-22	6.85E-01	7.57E-01
F3	Best	1.09E-74	1.07E-62	6.22E-02	3.44E+04	5.88E+00	2.02E+03
	Mean	3.75E-46	2.85E-06	1.73E+00	5.86E+04	4.04E+03	4.42E+03
	STD	1.68E-45	1.27E-05	4.01E+00	1.59E+04	4.51E+03	1.40E+03
F4	Best	2.38E-42	6.97E-36	2.17E-04	1.62E+00	3.60E-11	1.59E+00
	Mean	5.89E-28	4.59E-19	8.22E-04	6.20E+00	6.54E-05	2.53E+00
	STD	2.62E-27	2.02E-18	4.64E-04	2.32E+00	1.58E-04	2.99E-01
F5	Best	2.28E+01	2.71E+01	2.59E+01	2.78E+01	2.89E+01	3.27E+05
	Mean	2.36E+01	2.59E+01	2.79E+01	2.73E+01	1.69E+02	8.43E+05
	STD	3.60E-01	2.31E-01	6.54E-01	3.20E-01	2.18E+02	4.43E+05
F6	Best	2.57E-07	7.75E-04	8.71E-06	1.92E-01	5.45E+00	1.72E+03
	Mean	1.40E-05	9.48E-03	5.17E-01	5.49E-01	6.36E+00	3.54E+03
	STD	3.81E-05	1.22E-02	3.73E-01	2.42E-01	4.94E-01	1.16E+03
F7	Best	1.88E-04	1.52E-03	1.41E-03	1.67E-05	8.95E-04	1.74E-01
	Mean	7.84E-04	5.11E-03	4.53E-03	5.37E-03	1.47E-02	4.33E-01
	STD	6.19E-04	3.35E-03	2.17E-03	6.69E-03	1.45E-02	1.71E-01
F8	Best	3.74E-87	1.26E-69	1.71E-28	1.45E-40	7.01E-13	3.63E-01
	Mean	2.20E-63	2.84E-36	1.68E-26	6.47E-34	5.27E-06	6.94E+00
	STD	8.39E-63	1.27E-35	2.88E-26	2.82E-33	1.20E-05	5.62E+00
F9	Best	8.99E-42	1.19E-35	1.31E-15	4.26E-25	1.62E-11	8.70E-02
	Mean	8.98E-14	1.58E-05	2.41E-04	3.47E-01	6.74E-07	1.43E+00
	STD	3.53E-13	7.06E-05	2.33E-04	8.63E-01	1.13E-06	8.25E-01
F10	Best	1.13E-101	2.23E-82	1.67E-49	4.58E-62	1.83E-09	1.42E-06
	Mean	3.49E-86	3.14E-52	1.17E-40	2.68E-51	4.90E-07	6.85E-05
	STD	1.51E-85	1.23E-51	5.24E-40	1.19E-50	1.35E-06	1.11E-04
F11	Best	4.22E-82	2.34E-65	3.51E-08	1.82E-38	1.32E-05	6.59E+06
	Mean	2.06E-53	1.59E-32	3.88E-07	6.40E-27	2.29E+02	3.38E+07
	STD	9.13E-53	7.11E-32	4.65E-07	2.50E-26	6.63E+02	2.05E+07
F12	Best	6.10E-80	3.44E-70	3.05E-17	3.14E+00	1.64E+00	3.87E-01
	Mean	1.47E-55	4.35E-12	8.43E-15	8.33E+01	6.11E+00	4.49E+00
	STD	6.29E-55	1.95E-11	1.55E-14	4.91E+01	2.95E+00	2.49E+00
F13	Best	-9.53E+03	-1.05E+04	-8.11E+03	-1.26E+04	-9.66E+03	-4.58E+03
	Mean	-6.11E+03	-9.11E+03	-6.21E+03	-9.94E+03	-6.81E+03	-3.74E+03
	STD	2.49E+03	8.89E+02	1.18E+03	1.91E+03	1.48E+03	3.37E+02
F14	Best	0.00E+00	0.00E+00	2.84E-14	0.00E+00	0.00E+00	1.55E+01
	Mean	2.78E-11	1.49E+00	3.01E+00	4.68E+00	2.24E-06	3.12E+01
	STD	1.24E-10	4.64E+00	3.12E+00	1.02E+01	7.05E-06	9.47E+00
F15	Best	8.78E-16	8.78E-16	4.71E-14	8.79E-16	1.41E-10	4.38E+00
	Mean	8.88E-16	1.42E-15	3.18E-13	1.05E-14	3.66E-05	6.13E+00
	STD	0.00E+00	1.20E-15	3.08E-13	6.43E-15	6.87E-05	1.23E+00
F16	Best	0.00E+00	0.00E+00	0.00E+00	0.00E+00	1.44E-11	8.64E-01
	Mean	0.00E+00	3.46E-02	4.93E-02	1.51E-01	1.89E-04	2.40E+00
	STD	0.00E+00	5.87E-02	5.68E-02	1.91E-01	5.48E-04	1.27E+00
F17	Best	6.29E-09	1.63E-05	5.13E-03	8.76E-03	4.78E-01	1.20E+01
	Mean	2.12E-07	1.24E-03	3.03E-02	4.13E-02	1.58E+00	1.38E+03
	STD	1.81E-07	3.60E-03	1.70E-02	5.76E-02	1.63E+00	3.31E+03

TABLE 4. (Continued.) Benchmark function optimization results.

F18	Best	1.71E-07	1.43E-02	9.84E-02	3.05E-01	3.00E+00	6.79E+03
	Mean	1.08E-02	4.72E-01	4.28E-01	5.52E-01	5.78E+00	2.87E+05
	STD	1.25E-02	3.74E-01	2.27E-01	1.92E-01	3.69E+00	2.70E+05
F19	Best	1.47E+03	1.79E+03	4.78E+03	1.22E+00	3.87E+03	7.68E+03
	Mean	7.35E+03	3.82E+03	6.45E+03	2.27E+03	5.62E+03	8.66E+03
	STD	2.30E+03	1.28E+03	1.32E+03	1.89E+03	1.03E+03	5.24E+02
F20	Best	3.12E-04	4.29E-04	3.18E-04	3.34E-04	9.06E-04	3.20E-04
	Mean	3.06E-04	1.02E-03	7.49E-03	6.93E-04	6.94E-03	1.24E-03
	STD	4.98E-19	3.60E-04	9.72E-03	3.37E-04	8.51E-03	6.08E-04
F21	Best	-1.00E+00	-1.00E+00	-1.00E+00	-1.00E+00	-1.00E+00	-9.99E-01
	Mean	-1.00E+00	-1.00E+00	-1.00E+00	-9.90E-01	-1.00E+00	-9.83E-01
	STD	0.00E+00	0.00E+00	0.00E+00	2.34E-02	1.66E-08	1.88E-02
F22	Best	3.82E-105	4.41E-58	3.80E-58	8.05E-99	0.00E+00	1.81E-48
	Mean	1.52E-70	6.83E-42	6.30E-41	8.34E-78	1.17E-06	1.71E-21
	STD	6.26E-70	2.10E-41	2.70E-40	3.41E-77	1.83E-06	7.54E-21
F23	Best	0.00E+00	0.00E+00	0.00E+00	0.00E+00	0.00E+00	2.86E-05
	Mean	0.00E+00	3.07E-11	1.14E-02	2.62E-02	9.46E-08	1.85E-02
	STD	0.00E+00	1.26E-10	1.94E-02	2.20E-02	3.57E-07	1.62E-02

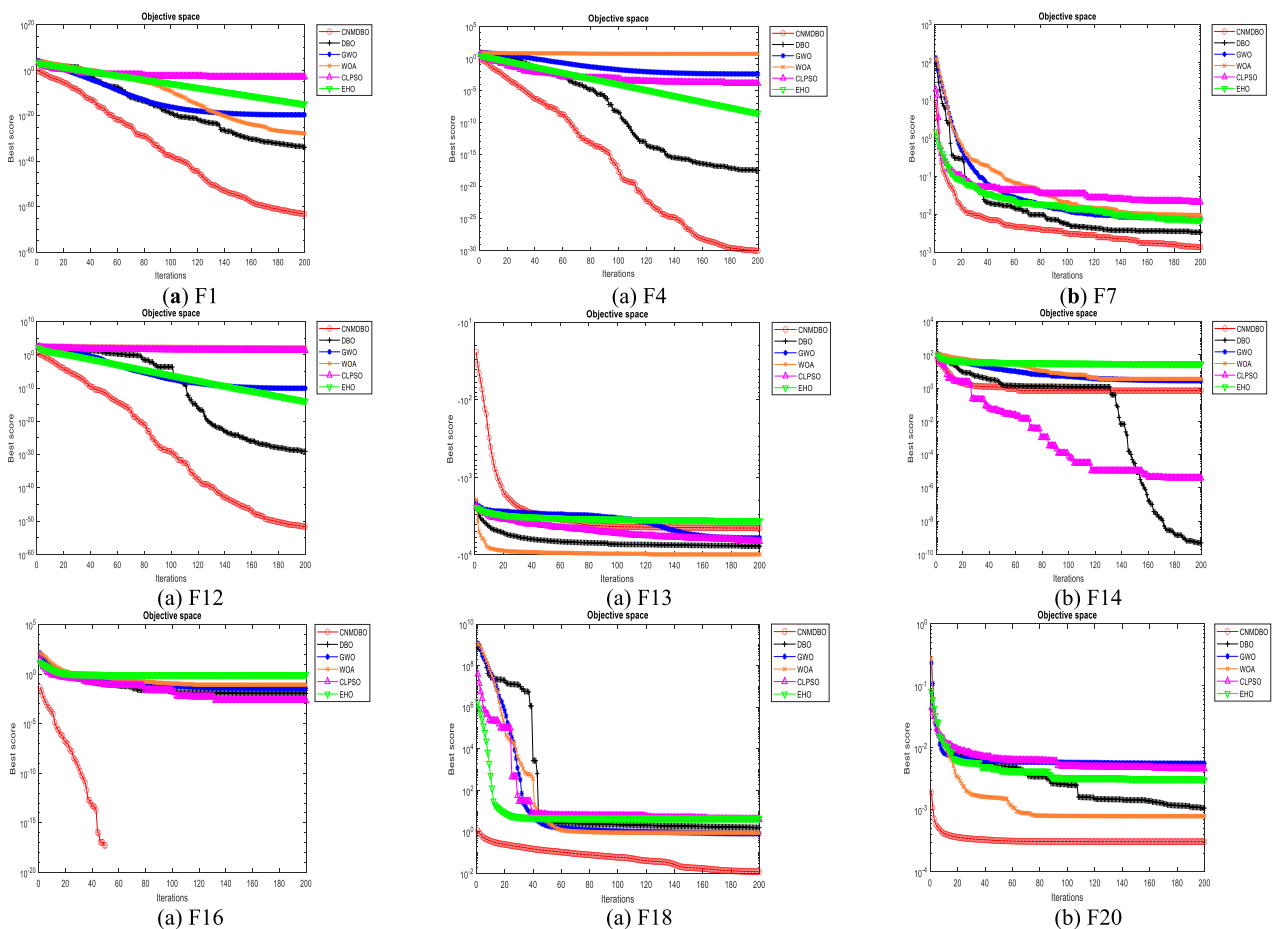


FIGURE 8. The IDBO method and other optimizers' convergence curves.

meta-heuristics methods: Elephant Herding Optimization (EHO) [40], Comprehensive Learning Particle Swarm Optimizer (CLPSO) [41], Grey Wolf Optimization (GWO) [42],

Whale Optimization Algorithm (WOA) [43] and DBO [28]. The details parameter settings of these optimization algorithms are shown in Table 3.

TABLE 5. Wilcoxon rank sum test.

Function	DBO	GWO	WOA	CLPSO	EHO
F1	1.44E-14 < 0.05	1.44E-14 < 0.05	1.44E-14 < 0.05	1.44E-14 < 0.05	1.44E-14 < 0.05
F2	1.44E-11 < 0.05	1.44E-14 < 0.05	1.44E-14 < 0.05	1.44E-14 < 0.05	1.44E-08 < 0.05
F3	1.32E-14 < 0.05	1.44E-13 < 0.05	1.44E-14 < 0.05	1.44E-14 < 0.05	1.61E-12 < 0.05
F4	1.44E-17 < 0.05	1.44E-14 < 0.05	3.02E-07 < 0.05	1.44E-14 < 0.05	1.44E-17 < 0.05
F5	1.83E-14 < 0.05	1.22E-12 < 0.05	1.44E-06 < 0.05	1.44E-14 < 0.05	1.44E-14 < 0.05
F6	1.47E-05 < 0.05	1.44E-14 < 0.05	1.44E-14 < 0.05	1.44E-16 < 0.05	1.79E-14 < 0.05
F7	1.00E-01	1.43E-214 < 0.05	1.43E-14 < 0.05	1.43E-14 < 0.05	1.43E-18 < 0.05
F8	1.21E-18 < 0.05	1.44E-14 < 0.05	1.44E-11 < 0.05	1.44E-14 < 0.05	2.79E-15 < 0.05
F9	1.44E-14 < 0.05	1.44E-08 < 0.05	1.44E-10 < 0.05	1.44E-14 < 0.05	1.44E-14 < 0.05
F10	1.21E-14 < 0.05	3.16E-14 < 0.05	1.44E-13 < 0.05	1.44E-14 < 0.05	5.36E-14 < 0.05
F11	1.44E-14 < 0.05	1.44E-14 < 0.05	1.44E-14 < 0.05	1.44E-14 < 0.05	1.44E-14 < 0.05
F12	2.49E-05 < 0.05	1.44E-14 < 0.05	2.15E-14 < 0.05	1.44E-03 < 0.05	4.63E-10 < 0.05
F13	3.25E-02 < 0.05	1.23E-04 < 0.05	6.23E-05 < 0.05	5.01E-02	1.23E-06 < 0.05
F14	1.44E-14 < 0.05	1.44E-14 < 0.05	1.44E-14 < 0.05	1.44E-14 < 0.05	1.44E-14 < 0.05
F15	1.44E-14 < 0.05	1.67E-14 < 0.05	1.44E-12 < 0.05	1.44E-11 < 0.05	1.44E-14 < 0.05
F16	2.77E-14 < 0.05	1.44E-14 < 0.05	9.11E-17 < 0.05	1.44E-12 < 0.05	1.44E-14 < 0.05
F17	1.44E-14 < 0.05	1.44E-14 < 0.05	1.44E-14 < 0.05	1.44E-14 < 0.05	3.54E-14 < 0.05
F18	1.65E-14 < 0.05	1.44E-19 < 0.05	1.44E-14 < 0.05	1.44E-14 < 0.05	1.44E-14 < 0.05
F19	5.98E-02	5.98E-04 < 0.05	7.30E-02	5.98E-04 < 0.05	5.98E-04 < 0.05
F20	1.44E-05 < 0.05	1.44E-14 < 0.05	1.44E-14 < 0.05	1.44E-14 < 0.05	3.51E-14 < 0.05
F21	1.36E-14 < 0.05	1.69E-17 < 0.05	1.36E-14 < 0.05	1.36E-14 < 0.05	1.36E-17 < 0.05
F22	1.29E-14 < 0.05	1.44E-14 < 0.05	1.44E-14 < 0.05	1.44E-09 < 0.05	1.01E-21 < 0.05
F23	1.44E-14 < 0.05	1.44E-14 < 0.05	1.44E-14 < 0.05	1.44E-06 < 0.05	1.44E-08 < 0.05

Maximum iterations are set at 200 and a uniform population size of 50 so that the IDBO method and its comparison algorithms can be evaluated more accurately. Moreover, each model was run independently twenty times, the dimensions were defined as 2, 4, 10, 30 and 50. So as to mitigate the impact of the random factor on the experiment, the most optimal values, standard deviations, averages, and of the optimization algorithm were recorded one by one for each simulation experiment.

MatlabR2022b was used to simulate the experiment on a Windows 10 operating system with an i7-13700 processor. IDBO and other classical optimization algorithms were tested in a standard test function to illustrate the validity by comparing the best value, mean value and standard errors of fitness.

C. ANALYSIS OF CONVERGENCE CURVES

Unimodal functions are very suitable for verifying the development abilities of algorithms in exploring optimal solutions. Meanwhile, multimodal functions can be used to evaluate IDBO's ability to evade local optimal solutions during exploration. The final results of the optimization method are presented in Table 4. The optimal solution is shown in boldface. Except for F13 and F19, IDBO is superior to other algorithms, and its Standard deviation, average value,

and optimal value are all optimal. It is apparent that the effectiveness of the IDBO is superior to that of the DBO, demonstrating that the suggested algorithm presented in this paper can enhance the search capability.

For more intuitive observation and comparison of the convergence speed, accuracy, and capacity to avoid local optima of each algorithm, Fig. 8 shows the convergence curves of IDBO and five basic meta-heuristics methods. The number of iterations is shown on the horizontal axis, and the magnitude of adaptation value is represented on the vertical axis. The adaptation value is expressed as a logarithm in base 10 to better illustrate the convergence trend.

According to Fig. 8, IDBO demonstrates the quickest convergence as well as the highest accuracy in the functions F1-F12, F15-F18, and F20-F23, this suggests that IDBO is more likely to find and converge to the global optimum, which is due to the circle chaotic mapping in population initialization stage, so that the distribution of dung beetles is more uniform than random distribution. For function F13, although IDBO is not the optimal solution, it has little difference from the results of other algorithms, it may be that noise is generated in the mutation process. For function F14, the performance is unstable, most of the time IDBO converges quickly at the inflection point and reaches optimal accuracy after iteration, and occasionally the result is the worst,

this is because the dynamic disturbance makes the IDBO algorithm exhibit strong ability in F14, F18 and some other functions. For function F19, IDBO obtains the optimal value after convergence, followed by WOA and IDBO, probably because it is trapped in a local optimum. In conclusion, the circle sequence, non-uniform Gaussian variation strategy, and multi-stage perturbation strategy effectively improve the IDBO algorithm's global and local optimization capabilities, indicating that the improved strategy suggested in this paper effectively enhances the convergence speed and accuracy.

D. WILCOXON RANK SUM TEST

To verify the effectiveness of IDBO, it is not enough to compare the convergence analysis, standard deviation and mean, we need to compare algorithm effectiveness at the statistical level such as the Wilcoxon statistical test [44], [45]. The Wilcoxon rank sum test is a nonparametric statistical test used to determine whether there are significant differences between IDBO and different algorithms, therefore, we tested each of the six algorithms 50 times independently on 23 test functions. The Wilcoxon rank sum test was performed at the significance level of 0.05 to determine the significant difference between the six compared algorithms and the solution results of IDBO. As shown in Tables 5, when the comparison result of the IDBO with other algorithms is less than 5%, it indicates that there is a noticeable variation. Conversely, when the comparison result is greater than 5%, the difference between the two algorithms is not noticeable. From Tables 4, it can be seen that the IDBO algorithm is different from the other algorithms. In summary, IDBO has a significant advantage over DBO, GWO, WOA, CLPSO, and EHO, so the superiority of the IDBO algorithm proposed in this paper is statistically significant.

E. SENSITIVITY ANALYSIS

This section illustrates the effect of different IDBO improvement strategies through sensitivity analysis. each function was run 20 times independently, and the average value was used to analyze the impact of not adopting the improvement strategy on IDBO. Specifically, IDBO1 does not use the circle chaotic mapping strategy in population initialization and will adopt the traditional population random deployment setup. In IDBO2, the proposed non-uniform Gaussian variational strategy is no longer used to perform mutation operations on the dung beetle with the worst fitness in the population, random selection is performed according to the original DBO. In IDBO3, the multi-stage dynamic disturbance strategy for each iteration is no longer used, and the resulting tests are shown in Table 6.

It can be seen from Table 6 that the performances in IDBO1 significantly decreases if the circle chaotic mapping strategy in population initialization is removed, which indicates that the circle chaotic mapping strategy serves a critical part in the features of the IDBO. While the IDBO2 has better

TABLE 6. IDBO and other formats run results.

Function	IDBO1	IDBO2	IDBO3	IDBO
F1	1.44E-32	6.78E-46	4.35 E-50	8.37E-66
F2	2.82E-19	4.28E-24	3.02E-26	2.17E-31
F3	1.32E-24	5.17E-29	3.51E-30	3.65E-45
F4	4.67E-10	1.06E-25	5.49E-24	5.89E-29
F5	6.95E+01	2.23E+01	1.15E+01	2.76E+01
F6	1.45E-02	1.56E-04	3.79E-04	1.55E-05
F7	6.93E-01	7.72E-03	4.63E-03	7.84E-04
F8	3.17E-30	2.75E-48	2.83E-50	2.26E-64
F9	5.17E-08	5.32E-12	6.60E-13	9.08E-15
F10	4.39E-41	6.06E-68	2.87E-65	3.52E-87
F11	3.01E-23	2.12E-35	1.54E-41	2.26E-54
F12	1.24E-19	3.51E-36	1.46E-40	1.58E-55
F13	-3.59E+03	-4.01E+03	-9.68E+03	-9.24E+03
F14	3.79E-04	6.25E-08	6.37E-09	2.67E-11
F15	6.61E-07	8.42E-12	2.17E-13	8.86E-15
F16	2.51E+00	1.81E+00	1.68E+00	0.00E+00
F17	2.74E-02	3.38E-05	3.97E-05	2.23E-07
F18	1.69E-01	1.12E-01	1.09E-01	1.18E-02
F19	4.97E+03	1.72E+03	3.66E+03	2.16E+03
F20	6.08E-02	4.68E-03	8.32E-03	3.06E-04
F21	-3.16E-01	-5.75E-01	-9.23E-01	-1.00E+00
F22	5.75E-32	6.66E-55	2.74E-62	1.53E-70
F23	2.06E+00	1.34E+00	1.01E+00	0.00E+00

convergence accuracy than IDBO1, probably non-uniform Gaussian variational maintains population diversity and enhances the global search ability of the algorithm. There is little difference in convergence between IDBO2 and IDBO3, probably multi-stage dynamic disturbance strategy in rolling ball may be prone to noise while updating the position of the optimal solution. This demonstrate that the effect of different strategies on algorithm performance improvement is also different, but if the three strategies are used at the same time, not only the accuracy is improved, but also improve the stability of the algorithm, proving that the improvement strategy has authenticity and effectiveness.

V. NLOS IDENTIFICATION EXPERIMENTAL RESEARCH

To verify the effectiveness of our proposed IDBO-CNN for NLOS identification, this section leverages UWB data collected from real-world environments to setup simulation experiments to evaluate NLOS identification performance.

A. DATA PRESENTATION AND PREPROCESSING

The dataset used in this paper comes from the elastic Wireless Networking Experimentation (eWINE) project, which uses a DWM1000 RF transceiver to collect indoor UWB signals. UWB signals in seven different environments,

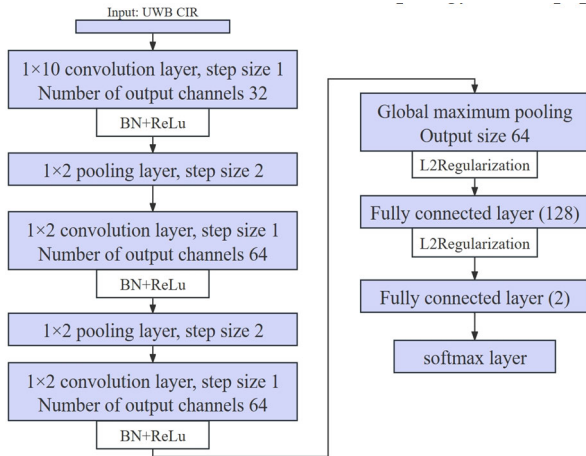


FIGURE 9. The proposed CNN structure and parameters in this paper.

collected 3000 LOS data and 3000 NLOS data for each scene. The dataset collected a total of 42000 data, including 21000 LOS and 21000 NLOS, more information can be found at <https://www.eWINE-project.eu/>. The dataset consists of 7 CSV format files, each of which stores 6000 UWB data collected in different scenarios. Each dataset file has 1024 columns of data, including whether it is an NLOS signal, 1016 CIR data from CIR0 to CIR1015, time of flight, noise standard deviation, length of leading code, and other characteristic data.

According to the tips of the eWINE project, the CIR data needs to be divided by the number of obtained leading code samples. In this paper, 7 data set files are processed by CIR data according to the tips of the eWINE project, and then the unused data is deleted, leaving only 1016 columns of data that need to be used. The CIR data is normalized to increase the training speed of the model, and the dataset in this paper was obtained through the above operations.

B. NETWORK STRUCTURE

When the input CIR signal is more complex, that is, more sample data are included in the CIR to be identified, in order to improve the recognition rate of NLOS, convolutional neural networks generally need to gain a deeper understanding of the input data by analyzing its more abstract and complex characteristics. In order to enable the CNN to learn more feature parameters, more layers are usually set reasonably in practice. This research utilized a CNN with an output layer, two fully-connected layers, three pooling layers, and three convolutional layers. Fig. 9 shows the proposed convolutional neural network topology in this paper.

The hierarchical distribution determines that CNN has many hyperparameters, and the hyperparameter optimization problem is to select an optimal hyperparameter collocation in the network model. For a given problem, it is difficult to know the best combination scheme of hyperparameters, it will cost many experimental and time to reproduce the values used in other problems by the previous empirical method or to

find the best values through repeated trials, and you may not obtain the optimal solution. Therefore, this paper proposes to IDBO based on circle sequence, non-uniform Gaussian variation strategy, and multi-stage perturbation strategy, and then optimize the parameters of CNN. The hyperparameter this study focuses on are as follows:

(1) BatchSize. The larger the BatchSize, the faster the training, the larger the memory usage, but the slower the convergence. Smaller batch sizes help to generalize performance, while larger ones can improve accuracy, speed.

(2) L2 Regularization. Larger values of L2 regularization parameter make the model more generalized, but setting the parameter too high will reduce the model fitting ability.

(3) Learning rate. If the learning rate is too low, it is easy for the model to fall into a local optimum, and if it is too high, it is easy to miss the global optimum and fail to complete the training.

The essence of IDBO-CNN is to adjust the hyperparameters of CNN near the optimal solution by using the faster convergence rate of IDBO and accurate global optimization ability. Thus, it can reduce the time of model construction and improve the accuracy of prediction. The position of each beetle is represented by a 3-dimensional vector $P_i(p_{i1}, p_{i2}, p_{i3})$, whose dimension is equal to the number of hyperparameters to be optimized. Specific optimization methods are as follows: the hyperparameter of the CNN model is used as the beetle's location parameter, the recognition rate of the CNN model is regarded as the fitness of the beetle at the current position. Then, let each beetle move to a new position according to the strategy in Section III-C. The beetle population is set to 50, and the number of searches is set to 30. After all searches are done, the beetle with the greatest fitness is selected, and its positional parameters represent the best hyperparameters.

C. ANALYSIS OF EXPERIMENTAL RESULTS

In this paper, six environments in the dataset (one of two office environments is selected) are selected for experiments, the dataset for each environment is separated into training and test sets, with 80% of the data assigned to the former and 20% to the latter. After IDBO optimization, the optimal initial learning rate is 0.2, the optimal L2 regularization coefficient is 0.1, the minimum batch size is set to 16, iterations are limited to 2000, the random gradient descent optimizer is used, and the contribution of update parameters from the previous iteration to the current iteration's random gradient descent is set to 0.9.

According to the parameters and model evaluation indexes set above, IDBO-CNN models belonging to 6 kinds of indoor scenes are trained, respectively. The training accuracy of scene 6 (the boiler room) is illustrated by the change curve in Fig. 10, which is progressively increasing over iterations. It can be seen that there is no overfitting phenomenon in the scenario 6 model, and the final F1 value is 90.96%.

TABLE 7. NLOS identification performance of IDBO-CNN in different scenarios.

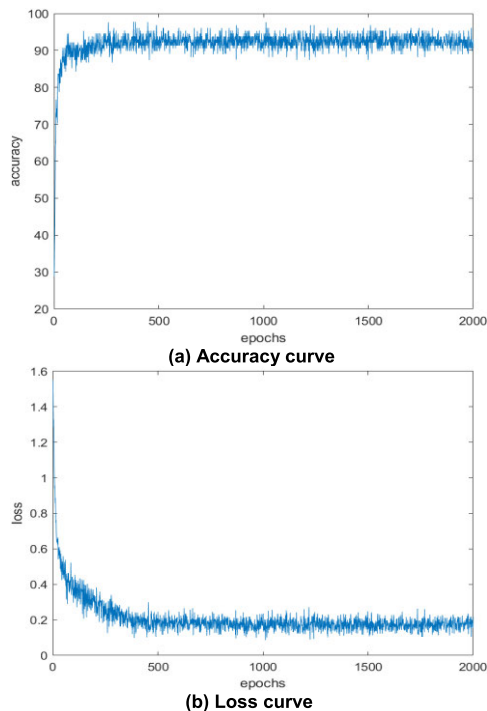
Algorithm	Accuracy (%)	Precision (%)	Recall (%)	F1 Score (%)
Office	90.50	96.51	83.83	89.72
Apartment	88.12	87.66	88.70	88.17
Workshop	87.23	86.13	88.26	87.18
Kitchen	86.20	85.34	87.90	87.75
Bedroom	90.91	90.43	91.50	90.96
Boiler room.	87.65	86.97	88.57	87.76

TABLE 8. Hyperparameter setting.

Hyperparameter	CNN1	CNN2	IDBO-CNN
Learning rate	0.05	0.4	0.2
L2 regularization coefficient	0.05	0.2	0.1
Batch size	10	20	16

TABLE 9. Comparison of NLOS identification performance between the suggested method and existing CNN methods.

Algorithm	Accuracy (%)	Precision (%)	Recall (%)	F1 Score (%)
CNN1	89.32	87.88	87.54	89.20
CNN2	88.73	86.34	88.54	87.65
IDBO-CNN	90.91	90.43	91.50	90.96

**FIGURE 10.** The curve of the training process: (a) Accuracy curve; (b) Loss curve.

Each of the six environments in the dataset has specific multipath propagation characteristics, thus increasing the robustness of the identification model. In this paper, the performance of six scene classification models was tested. Table 7 shows that the NLOS classification accuracy of all

six scenes reached more than 86%, from the overall classification performance, bedroom scene and office scene are better than other scenes, the workshop scene model has the worst classification performance. A rough estimate is that this dataset is affected by the multipath effect and NLOS during measurement, and the dataset lacks generalization ability, resulting in lower classification performance than other scenes.

To assess the NLOS classification performance of the IDBO-CNN model more accurately, a comparison test of the CNN classification model was set up. The experimental data set of scenario1 (office scene) is selected, Table 8 and Table 9 show the parameter Settings and experimental results respectively.

Table 9 shows that the accuracy the proposed method in scenario 6 is 90.91%, which performs better than traditional CNN method with 89.32% and 88.73% accuracy, it is also higher than the method proposed by Jiang et al. [46]. Therefore, in the same scene, by using the IDBO to optimize the parameters of CNN, the feature extraction ability and identification ability of the model for NLOS signals are improved, and the overall performance is better than the existing convolutional neural network recognition method with manually set parameters.

VI. CONCLUSION

The indoor positioning accuracy of UWB decreases in NLOS scenarios, and identifying NLOS can achieve better positioning accuracy. Aiming at the problem of NLOS identification in UWB positioning, this paper proposes a CNN classification algorithm based on multi-strategy

improved DBO. Firstly, based on the standard DBO, the Circle chaotic mapping, non-uniform Gaussian variational strategy, and multi-stage perturbation strategy are used to enhance the optimization performance of the DBO method, the superiority-seeking ability of IDBO is demonstrated by testing 23 different types of benchmark functions. In addition, based on the IDBO algorithm, we suggested an IDBO-CNN model to improve the NLOS identification effectiveness. Through the utilization of IDBO's quicker convergence time and more accurate global optimization capability, the hyper-parameters of CNN are tuned to reach the optimal solution, thereby enhance the precision of NLOS identification. The results of the simulation experiment show that IDBO-CNN achieves the expected effect in 6 different indoor scenes, and the F1 score is enhanced by 3.31% compared with the traditional CNN method, which proves that IDBO-CNN has better identification accuracy and robustness.

IDBO-CNN still has some shortcomings because the proposed algorithm in this paper is to train the respective signal identification models in different scenarios, and when one identification model is applied to another scenario, the NLOS signal identification effect is not ideal, in future work, we hope to realize an UWB NLOS signal identification model suitable for different scenarios and to enhance the model's robustness and identification accuracy.

REFERENCES

- [1] R. Chen, Z. Li, F. Ye, G. Guo, S. Xu, L. Qian, Z. Liu, and L. Huang, "Precise indoor positioning based on acoustic ranging in smartphone," *IEEE Trans. Instrum. Meas.*, vol. 70, pp. 1–12, 2021.
- [2] L. Hai, Z. Yang, Z. Cao, and M. Yang, "An improved weighted centroid localization algorithm based on Zigbee," in *Proc. 5th Int. Conf. Adv. Electron. Mater., Comput. Softw. Eng. (AEMCSE)*, Apr. 2022, pp. 634–637.
- [3] A. LaMarca and E. De Lara, *Location Systems: An Introduction to the Technology Behind Location Awareness*. Springer, 2022.
- [4] D. Vuong, T. Son, D. Ai, T.-H. Do, C. Huynh, H. N. Tan, N. Quang, and Ttvinh, "A novel integrated model for positioning indoor MISO VLC exploiting non-light-of-sight communication," in *Proc. 16th Int. Conf. Ubiquitous Inf. Manage. Commun. (IMCOM)*, Jan. 2022, pp. 1–5.
- [5] J. Xu, Z. Li, K. Zhang, J. Yang, N. Gao, Z. Zhang, and Z. Meng, "The principle, methods and recent progress in RFID positioning techniques: A review," *IEEE J. Radio Freq. Identificat.*, vol. 7, pp. 50–63, 2023.
- [6] Z. Niu, H. Yang, L. Zhou, M. F. Taha, Y. He, and Z. Qiu, "Deep learning-based ranging error mitigation method for UWB localization system in greenhouse," *Comput. Electron. Agricult.*, vol. 205, Feb. 2023, Art. no. 107573.
- [7] K. Yu, K. Wen, Y. Li, S. Zhang, and K. Zhang, "A novel NLOS mitigation algorithm for UWB localization in harsh indoor environments," *IEEE Trans. Veh. Technol.*, vol. 68, no. 1, pp. 686–699, Jan. 2019.
- [8] F. Zhu, K. Yu, Y. Lin, C. Wang, J. Wang, and M. Chao, "Robust LOS/NLOS identification for UWB signals using improved fuzzy decision tree under volatile indoor conditions," *IEEE Trans. Instrum. Meas.*, vol. 72, pp. 1–11, 2023.
- [9] Z. Fan, H. Chu, F. Wang, and J. Lu, "A new non-line-of-sight localization algorithm for wireless sensor network," in *Proc. IEEE 6th Int. Conf. Comput. Commun. (ICCC)*, Dec. 2020, pp. 858–862.
- [10] M. Dong, "A low-cost NLOS identification and mitigation method for UWB ranging in static and dynamic environments," *IEEE Commun. Lett.*, vol. 25, no. 7, pp. 2420–2424, Jul. 2021.
- [11] Y. Wang, K. Gu, Y. Wu, W. Dai, and Y. Shen, "NLOS effect mitigation via spatial geometry exploitation in cooperative localization," *IEEE Trans. Wireless Commun.*, vol. 19, no. 9, pp. 6037–6049, Sep. 2020.
- [12] X. Shi, Y. H. Chew, C. Yuen, and Z. Yang, "A RSS-EKF localization method using HMM-based LOS/NLOS channel identification," in *Proc. IEEE Int. Conf. Commun. (ICC)*, Jun. 2014, pp. 160–165.
- [13] M. Mallik, A. K. Panja, and C. Chowdhury, "Paving the way with machine learning for seamless indoor-outdoor positioning: A survey," *Inf. Fusion*, vol. 94, pp. 126–151, Jun. 2023.
- [14] A. Musa, G. D. Nugraha, H. Han, D. Choi, S. Seo, and J. Kim, "A decision tree-based NLOS detection method for the UWB indoor location tracking accuracy improvement," *Int. J. Commun. Syst.*, vol. 32, no. 13, p. e3997, 2019.
- [15] H. Yang, Y. Wang, C. K. Seow, M. Sun, M. Si, and L. Huang, "UWB sensor-based indoor LOS/NLOS localization with support vector machine learning," *IEEE Sensors J.*, vol. 23, no. 3, pp. 2988–3004, Feb. 2023.
- [16] Y. Yang, L. Zhang, J. Xu, D. Li, J. Bao, and J. Tan, "Cooperative indoor localization system based UWB and random forest algorithm in complicated underground NLOS scenario," in *Proc. 9th Int. Conf. Digit. Home (ICDH)*, Oct. 2022, pp. 271–276.
- [17] F. Che, W. B. Abbas, Q. Z. Ahmed, B. Amjad, F. A. Khan, and P. I. Lazaridis, "Weighted naive Bayes approach for imbalanced indoor positioning system using UWB," in *Proc. IEEE Int. Black Sea Conf. Commun. Netw. (BlackSeaCom)*, Jun. 2022, pp. 72–76.
- [18] M. Stahlke, S. Kram, C. Mutschler, and T. Mahr, "NLOS detection using UWB channel impulse responses and convolutional neural networks," in *Proc. Int. Conf. Localization GNSS (ICL-GNSS)*, Jun. 2020, pp. 1–6.
- [19] P. Li, Y. Yan, Y. Tan, and H. Wang, "A novel temporal convolutional network for NLOS identification of UWB signal," in *Proc. 9th Int. Forum Electr. Eng. Autom. (IFEAA)*, 2022, pp. 373–376.
- [20] D.-H. Kim, A. Farhad, and J.-Y. Pyun, "UWB positioning system based on LSTM classification with mitigated NLOS effects," *IEEE Internet Things J.*, vol. 10, no. 2, pp. 1822–1835, Jan. 2023.
- [21] V.-H. Nguyen, M.-T. Nguyen, J. Choi, and Y.-H. Kim, "NLOS identification in WLANs using deep LSTM with CNN features," *Sensors*, vol. 18, no. 11, p. 4057, Nov. 2018.
- [22] Z. Cui, Y. Gao, J. Hu, S. Tian, and J. Cheng, "LOS/NLOS identification for indoor UWB positioning based on Morlet wavelet transform and convolutional neural networks," *IEEE Commun. Lett.*, vol. 25, no. 3, pp. 879–882, Mar. 2021.
- [23] H. Wang, Y. Tan, and P. Li, "A NLOS identification algorithm of UWB signal via temporal convolutional neural network and attention mechanism," Res. Square, Tech. Rep., 2022.
- [24] Y. Zhao and M. Wang, "The LOS/NLOS classification method based on deep learning for the UWB localization system in coal mines," *Appl. Sci.*, vol. 12, no. 13, p. 6484, Jun. 2022.
- [25] T. Chang, S. Jiang, Y. Sun, A. Jia, and W. Wang, "Multi-bandwidth NLOS identification based on deep learning method," in *Proc. 15th Eur. Conf. Antennas Propag. (EuCAP)*, Mar. 2021, pp. 1–5.
- [26] D. H. Tran, B. Chung, and Y. M. Jang, "GAN-based data augmentation for UWB NLOS identification using machine learning," in *Proc. Int. Conf. Artif. Intell. Inf. Commun. (ICAIIIC)*, Feb. 2022, pp. 417–420.
- [27] Q. Yuan, L. Wu, Y. Huang, Z. Guo, and N. Li, "Water-body detection from spaceborne SAR images with DBO-CNN," *IEEE Geosci. Remote Sens. Lett.*, vol. 20, pp. 1–5, 2023.
- [28] J. Xue and B. Shen, "Dung beetle optimizer: A new meta-heuristic algorithm for global optimization," *J. Supercomput.*, vol. 79, no. 7, pp. 7305–7336, May 2023.
- [29] X. Guo, X. Qin, Q. Zhang, Y. Zhang, P. Wang, and Z. Fan, "Speaker recognition based on dung beetle optimized CNN," *Appl. Sci.*, vol. 13, no. 17, p. 9787, Aug. 2023.
- [30] K. Zhao, D. Guo, M. Sun, C. Zhao, and H. Shuai, "Short-term traffic flow prediction based on VMD and IDBO-LSTM," *IEEE Access*, vol. 11, pp. 97072–97088, 2023.
- [31] R. Zhang and Y. Zhu, "Predicting the mechanical properties of heat-treated woods using optimization-algorithm-based BPNN," *Forests*, vol. 14, no. 5, p. 935, May 2023.
- [32] Y. Zhang, T. Ma, T. Li, and Y. Wang, "Short-term load forecasting based on DBO-LSTM model," in *Proc. 3rd Int. Conf. Energy Eng. Power Syst. (EEPS)*, Jul. 2023, pp. 972–977.
- [33] Y. Yan, M. Hongzhong, and L. Zhendong, "An improved grasshopper optimization algorithm for global optimization," *Chin. J. Electron.*, vol. 30, no. 3, pp. 451–459, May 2021.

- [34] Y. Wang, S. Chen, and Y. Wang, "Chaos encryption algorithm based on Kent mapping and AES combination," in *Proc. Int. Conf. Netw., Commun., Comput. Eng. (NCCE)*, 2018, pp. 588–592.
- [35] N. Li and W. Wang, "Prediction of mechanical properties of thermally modified wood based on TSSA-BP model," *Forests*, vol. 13, no. 2, p. 160, Jan. 2022.
- [36] Q. Wu, "A self-adaptive embedded chaotic particle swarm optimization for parameters selection of Wv-SVM," *Expert Syst. Appl.*, vol. 38, no. 1, pp. 184–192, Jan. 2011.
- [37] F. Zhu, G. Li, H. Tang, Y. Li, X. Lv, and X. Wang, "Dung beetle optimization algorithm based on quantum computing and multi-strategy fusion for solving engineering problems," *Expert Syst. Appl.*, vol. 236, Feb. 2024, Art. no. 121219.
- [38] X. Song, M. Zhao, Q. Yan, and S. Xing, "A high-efficiency adaptive artificial bee colony algorithm using two strategies for continuous optimization," *Swarm Evol. Comput.*, vol. 50, Nov. 2019, Art. no. 100549.
- [39] X.-S. He, W.-J. Ding, and X.-S. Yang, "Bat algorithm based on simulated annealing and Gaussian perturbations," *Neural Comput. Appl.*, vol. 25, no. 2, pp. 459–468, Aug. 2014.
- [40] G.-G. Wang, S. Deb, and L. d. S. Coelho, "Elephant herding optimization," in *Proc. 3rd Int. Symp. Comput. Bus. Intell. (ISCBI)*, Dec. 2015, pp. 1–5.
- [41] J. J. Liang, A. K. Qin, P. N. Suganthan, and S. Baskar, "Comprehensive learning particle swarm optimizer for global optimization of multimodal functions," *IEEE Trans. Evol. Comput.*, vol. 10, no. 3, pp. 281–295, Jun. 2006.
- [42] S. Mirjalili, S. M. Mirjalili, and A. Lewis, "Grey wolf optimizer," *Adv. Eng. Softw.*, vol. 69, pp. 46–61, Mar. 2014.
- [43] S. Mirjalili and A. Lewis, "The whale optimization algorithm," *Adv. Eng. Softw.*, vol. 95, pp. 51–67, Feb. 2016.
- [44] J. Carrasco, S. García, M. M. Rueda, S. Das, and F. Herrera, "Recent trends in the use of statistical tests for comparing swarm and evolutionary computing algorithms: Practical guidelines and a critical review," *Swarm Evol. Comput.*, vol. 54, May 2020, Art. no. 100665.
- [45] L. Li, L. Liu, Y. Shao, X. Zhang, Y. Chen, C. Guo, and H. Nian, "Enhancing swarm intelligence for obstacle avoidance with multi-strategy and improved dung beetle optimization algorithm in mobile robot navigation," *Electronics*, vol. 12, no. 21, p. 4462, 2023.
- [46] C. Jiang, J. Shen, S. Chen, Y. Chen, D. Liu, and Y. Bo, "UWB NLOS/LOS classification using deep learning method," *IEEE Commun. Lett.*, vol. 24, no. 10, pp. 2226–2230, Oct. 2020.



QIANKUN KONG was born in Shangqiu, Henan, China, in June 1993. He received the M.Sc. degree in electronics and communication engineering from the School of Communication Engineering, Chongqing University, in 2019. He is currently an Engineer with the Wuxi River Water Diversion Project Management Center. Indoor positioning is one of his study focuses. He was awarded the Qualification of Senior Engineer of Computer and Software Professional Technology by the Ministry of Industry and Information Technology of China.

• • •